Numerical convergence of the self-diffusion coefficient and viscosity obtained with Thomas-Fermi-Dirac molecular dynamics

J.-F. Danel, L. Kazandjian,* and G. Zérah
CEA, DAM, DIF, F-91297 Arpajon, France
(Received 27 January 2012; published 4 June 2012)

Computations of the self-diffusion coefficient and viscosity in warm dense matter are presented with an emphasis on obtaining numerical convergence and a careful evaluation of the standard deviation. The transport coefficients are computed with the Green-Kubo relation and orbital-free molecular dynamics at the Thomas-Fermi-Dirac level. The numerical parameters are varied until the Green-Kubo integral is equal to a constant in the $t \to +\infty$ limit; the transport coefficients are deduced from this constant and not by extrapolation of the Green-Kubo integral. The latter method, which gives rise to an unknown error, is tested for the computation of viscosity; it appears that it should be used with caution. In the large domain of coupling constant considered, both the self-diffusion coefficient and viscosity turn out to be well approximated by simple analytical laws using a single effective atomic number calculated in the average-atom model.

DOI: 10.1103/PhysRevE.85.066701 PACS number(s): 02.60.−x, 52.65.−y, 52.25.Fi

I. INTRODUCTION

Viscosity and mutual diffusion are important input properties for treating the problem of interface stability which can occur in particular in high-density high-temperature plasmas [1]. A first step toward improving the computation of these transport coefficients is to address self-diffusion and viscosity of pure elements in the same thermodynamic conditions. High-density high-temperature plasmas are in a thermodynamic state where they are a complex mixture of various particles (atoms, ions, electrons, molecules in a transient state). In such a situation where it is not possible to describe the particles and their interactions *a priori*, first-principles simulations, regarding a plasma as a mixture of electrons and nuclei, are highly useful to predict transport coefficients.

In quantum molecular dynamics (QMD), which treats the nuclei classically and the electrons quantum mechanically through finite-temperature density-functional theory [2], the only approximation lies in the exchange-correlation functional. QMD has been used for the determination of self-diffusion coefficients and viscosities [1,3–8]. Unfortunately, because of the Fermi-Dirac distribution of electronic quantum states, QMD is generally restricted to relatively low temperatures. In order to avoid the above limitation in the high-temperature regime, it is possible, with a semiclassical treatment of electrons (and a classical treatment of nuclei, as with QMD), to use orbital-free molecular dynamics (OFMD) in which the kinetic electronic free energy is a local functional of the electronic density. OFMD can be used at high temperature and, being orbital free, is relatively computationally cheap. When the exchange-correlation contribution is taken into account in the local-density approximation and the kinetic electronic free energy is expressed with the Thomas-Fermi approximation [9,10], OFMD is generally said to be applied at the Thomas-Fermi-Dirac level and gives rise to Thomas-Fermi-Dirac molecular dynamics (TFDMD); if the exchange-correlation contribution is omitted, the approach is called Thomas-Fermi molecular dynamics (TFMD).

TFMD was first used by Zérah *et al.* [11] to determine self-diffusion coefficients of hydrogen. More recently, TFDMD has been used to calculate self-diffusion coefficients and viscosities of heavier elements and of mixtures [1,7,8,12–14]. They are generally calculated through the Green-Kubo relation. Unlike the self-diffusion coefficient, whose statistical accuracy is improved by averaging over the particles, viscosity depends on the entire system and needs long simulations to gain statistical accuracy. In order to shorten the length of simulations, some authors [1,7,8] have proposed to extrapolate the off-diagonal stress tensor autocorrelation function in the $t \to +\infty$ limit, which leads to an unknown error for the viscosity; the same procedure is also sometimes applied to the self-diffusion coefficient [1]. The main purpose of this paper is to revisit the numerical convergence of the self-diffusion coefficient and viscosity and to show, in the framework of TFDMD and in a large domain of coupling constant, that these transport coefficients and their statistical errors can be computed without any extrapolation process. The results thus obtained will be compared to simple analytical models.

The remainder of this paper is organized as follows. Section II describes the TFDMD formalism and the prescriptions for computing the transport coefficients. Section III indicates how numerical convergence is obtained, presents various graphs of variation of the transport coefficients with respect to the numerical parameters, and provides a few tests of the extrapolation approach. Section IV compares the results obtained to those given by simple analytical models. Section V presents our conclusions. Atomic units are used unless otherwise stated.

II. FORMALISM

A. Thomas-Fermi-Dirac molecular dynamics

Simulations by TFDMD are performed with the electronic structure package ABINIT [15,16]. The system is constructed by replication of a finite sample of N atoms in a basic cubic reference cell. The dynamics of the nuclei, located at the position vectors $\mathbf{R}_i$, is driven by nuclear Coulomb interactions and by an effective potential $F_e[n(\mathbf{r}); \{\mathbf{R}_i\}]$ equal to the

*Corresponding author: luc.kazandjian@cea.fr

electronic free energy [13]; for given $\mathbf{R}_i$'s and thermodynamic conditions, F_e is a functional of the electronic density $n(\mathbf{r})$. In the Thomas-Fermi-Dirac method, at given volume V, temperature T, and position vectors $\mathbf{R}_i$, the electronic density is obtained by minimizing the following functional under the constraint of charge neutrality:

$$F_e[n(\mathbf{r});\{\mathbf{R}_i\}] = \int \mathcal{F}_0(n)d\mathbf{r} + \int \mathcal{F}_{xc}(n)d\mathbf{r} + \frac{1}{2}\iint \frac{n(\mathbf{r})n(\mathbf{r}')}{|\mathbf{r}-\mathbf{r}'|}\,d\mathbf{r}\,d\mathbf{r}' + \int n(\mathbf{r})v(\mathbf{r})d\mathbf{r}, \tag{1}$$

where $\mathcal{F}_0(n)$ is the kinetic electronic free energy per unit volume at electronic density n, $\mathcal{F}_{xc}(n)$ is the exchange-correlation contribution to the free energy per unit volume, and $v(\mathbf{r})$ is the external potential acting on the electrons (in the present case, it is due to the nuclei). $\mathcal{F}_{xc}(n)$ is taken equal to the sum of the exchange energy of the electron gas at $T = 0$ K [10] and of the correlation energy of the unpolarized electron gas at $T = 0$ K proposed by Perdew and Zunger [17].

At each time step, for given $\mathbf{R}_i$'s, the local electronic density is obtained by minimizing $F_e[n;\{\mathbf{R}_i\}]$ under the constraint of charge neutrality, and the forces acting on the nuclei are computed. The nuclei are then moved in the isokinetic ensemble [18,19]; other statistical ensembles can be used but the isokinetic ensemble allows one to regard temperature as exactly known. For given $\mathbf{R}_i$'s, the stress tensor is obtained as the derivative of the total free energy with respect to strain, as explained by Nielsen and Martin [20], with due simplification of the kinetic term in the Thomas-Fermi framework.

In the ABINIT code, electronic density is expressed as an expansion on a periodic plane-wave basis; the number of terms in this expansion is chosen with the cutoff energy e_{cut}. The divergence of the electronic density in the neighborhood of the nuclei is suppressed by replacing the Coulombic nucleus-electron interaction by a regularized potential constructed, at each thermodynamic condition, as explained by Lambert *et al.* [21]; as a result, the nucleus-electron interaction is no longer Coulombic below the cutoff radius r_{cut} and it must be verified that, as r_{cut} is lowered, a result independent of r_{cut} is obtained [22]. Besides the cutoff energy e_{cut} and the cutoff radius r_{cut} characterizing the regularized potential, the main numerical parameters intervening in the ABINIT code are the convergence parameter δE_{tol} for the minimization of F_e, the time step Δt used to displace the nuclei, the number n_{step} of time steps of the simulation (after the system has reached an equilibrium), and the number N of nuclei in the basic reference cell [22].

B. Transport properties

The self-diffusion coefficient is computed from the velocity autocorrelation function by the Green-Kubo formula

$$D = \lim_{t\to+\infty} D_{\text{GK}}(t), \tag{2}$$

$$D_{\text{GK}}(t) = \frac{1}{3N}\sum_{i=1}^{N}\int_0^t < \mathbf{v}_i(\tau)\cdot\mathbf{v}_i(0) > \, d\tau, \tag{3}$$

where $\mathbf{v}_i(\tau)$ is the velocity of nucleus i at time τ, and an average over the particles is performed to improve statistical precision [23]. In Eq. (3) and in Eq. (5) below, we use the angular bracket notation to represent an average over many time origins with each origin taken from a system at equilibrium [23].

The viscosity η is computed from the autocorrelation function of the off-diagonal components of the stress tensor by the Green-Kubo formula [23,24]

$$\eta = \lim_{t\to+\infty} \eta_{\text{GK}}(t), \tag{4}$$

$$\eta_{\text{GK}}(t) = \frac{1}{3Vk_BT}\sum_{\alpha>\beta}\int_0^t < \sigma_{\alpha\beta}(\tau)\,\sigma_{\alpha\beta}(0) > \, d\tau, \tag{5}$$

$$\sigma_{\alpha\beta}(t) = \sum_{i=1}^{N} m_i\, v_{i\alpha}(t)\, v_{i\beta}(t) + \sum_{i=1}^{N} R_{i\alpha}(t)\, f_{i\beta}(t), \tag{6}$$

where m_i is the mass of nucleus i, $v_{i\alpha}$ is the α component of $\mathbf{v}_i$, $R_{i\alpha}$ is the α component of the position vector $\mathbf{R}_i$ of nucleus i, $f_{i\beta}$ is the β component of the force $\mathbf{f}_i$ exerted on nucleus i, V is the volume of the basic cell, k_B is the Boltzmann constant, and T is the temperature. The stress tensor involves the entire system and not only one particle; as a result, unlike the case of self-diffusion, the statistical precision of viscosity cannot be improved by averaging over the N nuclei.

The practical computation of $D_{\text{GK}}(t)$ and $\eta_{\text{GK}}(t)$ is now described. The trajectory of length $(n_{\text{step}}-1)\Delta t$ taken into account in the calculation of $D_{\text{GK}}(t)$ and $\eta_{\text{GK}}(t)$ is obtained after an equilibration phase of 2000 time steps. $X_D(k\Delta t; n\Delta t)$ and $X_\eta(k\Delta t; n\Delta t)$ are defined by

$$X_D(k\Delta t; n\Delta t) = \frac{1}{3N}\sum_{i=1}^{N}\int_0^{n\Delta t} \mathbf{v}_i(\tau + k\Delta t)\cdot\mathbf{v}_i(k\Delta t)\,d\tau, \tag{7}$$

$$X_\eta(k\Delta t; n\Delta t) = \frac{1}{3Vk_BT}\sum_{\alpha>\beta}\int_0^{n\Delta t} \sigma_{\alpha\beta}(\tau + k\Delta t)\,\sigma_{\alpha\beta}(k\Delta t)\,d\tau, \tag{8}$$

where k and n are positive integers and the integrals are calculated with the trapezoidal rule.

$D_{\text{GK}}(t)$ and $\eta_{\text{GK}}(t)$ are computed with two-stage sampling [23]: For $Y = D$ or η and for a given n, the $X_Y(k\Delta t; n\Delta t)$ are divided into M equally long consecutive segments and the value retained for each segment is the average of the original values. If the segments are sufficiently long, $D_{\text{GK}}(t)$ and $\eta_{\text{GK}}(t)$ are thus sought from a random sample of M results. As a result of two-stage sampling, the computation of $D_{\text{GK}}(t)$ and $\eta_{\text{GK}}(t)$ is performed as follows:

$$Y_{\text{GK}}(n\Delta t) = \frac{1}{n_{\text{step2}}}\sum_{k=0}^{n_{\text{step2}}-1} X_Y(k\Delta t; n\Delta t), \tag{9}$$

where $Y = D$ or η depending on whether D or η is calculated, and a single value of n_{step2} is used for all n [so that the statistical accuracy of $Y_{\text{GK}}(n\Delta t)$ does not depend on n through n_{step2}]. We have chosen $n_{\text{step2}} = n_{\text{step}}/2$ (which implies $n < n_{\text{step}}/2$).

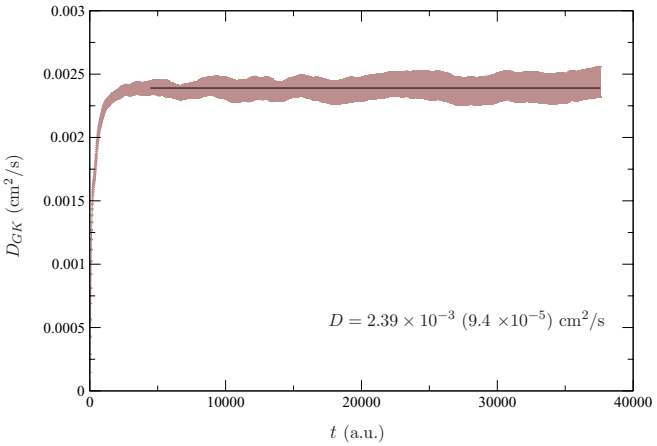

FIG. 1. (Color online) $D_{\mathrm{GK}}(t)$ for B_1. The numerical parameters are $N = 300$, $\Delta t = 12.53$ a.u., $e_{\mathrm{cut}} = 50$ Ha, $\delta E_{\mathrm{tol}} = 0.28$ Ha, $r_{\mathrm{cut}} = 0.54\, r_{\mathrm{WS}}$, and $n_{\mathrm{step}} = 6000$. The horizontal line indicates the domain of time used to calculate D and its standard deviation (written in parentheses). The error bars, representing the standard deviation, are displayed at each t (hence the area around the curve).

The standard deviation resulting from the above two-stage sampling is [23]

$$\sigma[Y_{\mathrm{GK}}(n\Delta t)] = \frac{1}{\sqrt{M(M-1)}} \sqrt{\sum_{j=1}^{M} [Y_{\mathrm{GK}}(n\Delta t) - Z_j(n\Delta t)]^2}, \tag{10}$$

$$Z_j(n\Delta t) = \frac{1}{L} \sum_{k=k_{\mathrm{inf}}(j)}^{k=k_{\mathrm{sup}}(j)} X_Y(k\Delta t; n\Delta t), \tag{11}$$

where L $[L = k_{\mathrm{sup}}(j) - k_{\mathrm{inf}}(j) + 1]$ is the number of time steps (calculated for each n) in a segment, $k_{\mathrm{inf}}(j)$ is the first time step of segment j, and $k_{\mathrm{sup}}(j)$ is the last time step of segment j. The length of the segments, and therefore the value of M, is evaluated at each n by computing a time correlation function of the $X_Y(k\Delta t; n\Delta t)$, with $0 \leqslant k < n_{\mathrm{step2}}$, and retaining the time at which the correlation function first cancels.

III. RESULTS

We apply the formalism described above to the cases given in Table I. B_1 and B_2 designate Boron 10 at two different thermodynamic conditions. We focus on B_1 for the presentation of the numerical convergence of the self-diffusion coefficient and on Cu for the numerical convergence of viscosity. The coupling constant Γ is defined by

$$\Gamma = \frac{Z^2}{r_{\mathrm{WS}} k_B T}, \tag{12}$$

where Z is the atomic number and the Wigner-Seitz radius r_{WS} is

$$r_{\mathrm{WS}} = \left(\frac{3}{4\pi n_i}\right)^{1/3}, \tag{13}$$

where n_i is the number density of atoms.

TABLE I. Cases for which the self-diffusion coefficient and viscosity are computed. Z is the atomic number, A is the atomic mass, ρ is the density, T is the temperature, and Γ is the coupling constant.

Element	Z	A (g/mole)	ρ (g/cm^3)	T(eV)	Γ
B_1	5	10.013	10	5	98.0
B_2	5	10.013	1	5	45.5
Cu	29	63.546	67.4	100	168
D	1	2.014	1.5	2.5	7.11

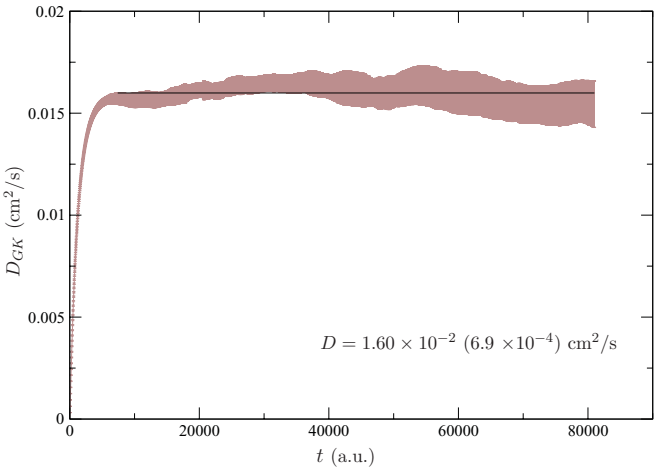

FIG. 2. (Color online) $D_{\mathrm{GK}}(t)$ for B_2. The numerical parameters are $N = 300$, $\Delta t = 27$ a.u., $e_{\mathrm{cut}} = 40$ Ha, $\delta E_{\mathrm{tol}} = 0.02$ Ha, $r_{\mathrm{cut}} = 0.35\, r_{\mathrm{WS}}$, and $n_{\mathrm{step}} = 6000$. The horizontal line indicates the domain of time used to calculate D and its standard deviation (written in parentheses). The error bars, representing the standard deviation, are displayed at each t (hence the area around the curve).

A. Self-diffusion coefficient

The function $D_{\mathrm{GK}}(t)$ is expected to be a constant in the $t \to +\infty$ limit, and this constant is equal to the

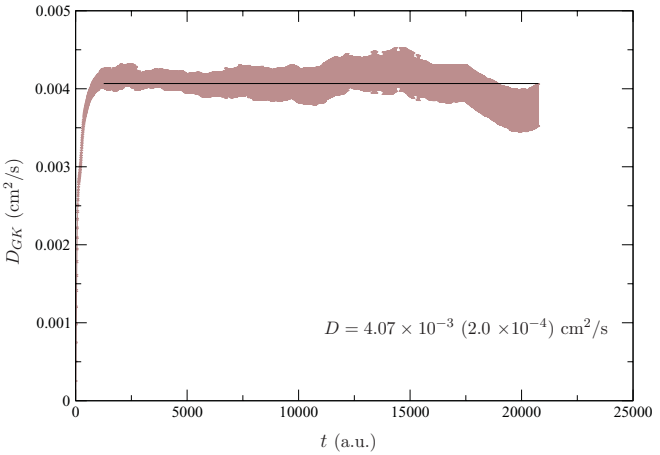

FIG. 3. (Color online) $D_{\mathrm{GK}}(t)$ for Cu. The numerical parameters are $N = 200$, $\Delta t = 6.92$ a.u., $e_{\mathrm{cut}} = 100$ Ha, $\delta E_{\mathrm{tol}} = 10^{-6}$ Ha, $r_{\mathrm{cut}} = 0.37\, r_{\mathrm{WS}}$, and $n_{\mathrm{step}} = 6000$. The horizontal line indicates the domain of time used to calculate D and its standard deviation (written in parentheses). The error bars, representing the standard deviation, are displayed at each t (hence the area around the curve).

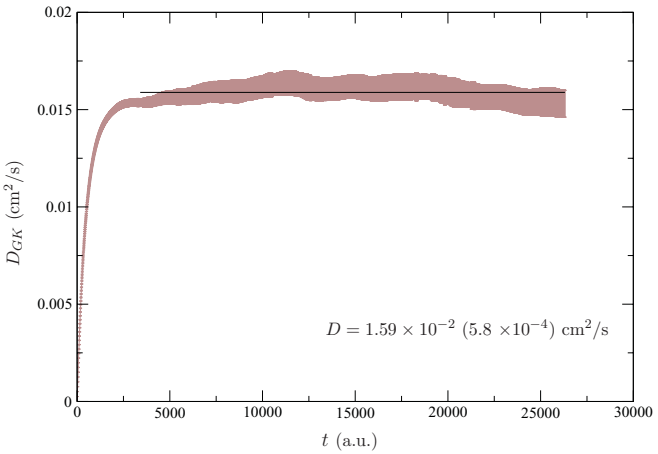

FIG. 4. (Color online) $D_{\mathrm{GK}}(t)$ for D. The numerical parameters are $N = 300$, $\Delta t = 8.77$ a.u., $e_{\mathrm{cut}} = 30$ Ha, $\delta E_{\mathrm{tol}} = 10^{-4}$ Ha, $r_{\mathrm{cut}} = 0.59\, r_{\mathrm{WS}}$, and $n_{\mathrm{step}} = 6000$. The horizontal line indicates the domain of time used to calculate D and its standard deviation (written in parentheses). The error bars, representing the standard deviation, are displayed at each t (hence the area around the curve).

self-diffusion coefficient D. All the numerical parameters evoked in Sec. II are determined by a systematic search for numerical convergence, that is, for a situation where, in the $t \to +\infty$ limit, a plateau independent of the parameters (within one standard deviation) is obtained. The initial parameters e_{cut}, r_{cut}, and Δt used in this search are determined by the rules of thumb described in Ref. [22] for the calculation of the thermodynamic properties (but numerical convergence is assessed in relation to the quantity computed only, as it should be). As r_{cut} and N are physical characteristics of the system (characterizing nucleus-electron interaction and periodicity), we start our search of the right parameters at given r_{cut} and N; then we let r_{cut} and N vary with the other parameters fixed. When the parameters are varied, the same set of initial positions and velocities is used, and the independence (within one standard deviation) of the self-diffusion coefficient to the choice of this set is verified.

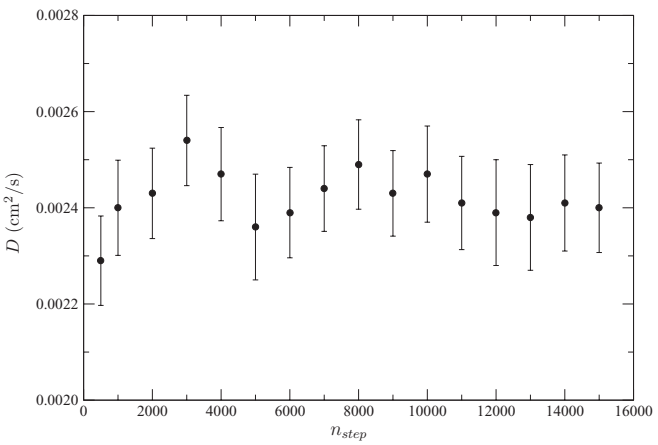

FIG. 5. Variation of the self-diffusion coefficient D with respect to n_{step} for B_1. The numerical parameters are $N = 300$, $\Delta t = 12.53$ a.u., $e_{\mathrm{cut}} = 50$ Ha, $\delta E_{\mathrm{tol}} = 0.28$ Ha, and $r_{\mathrm{cut}} = 0.54\, r_{\mathrm{WS}}$. The error bars represent the standard deviation.

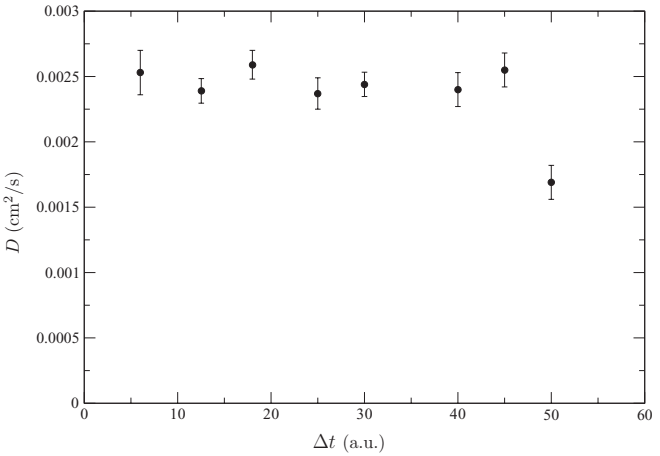

FIG. 6. Variation of the self-diffusion coefficient D with respect to the time step Δt for B_1. The numerical parameters are $N = 300$, $e_{\mathrm{cut}} = 50$ Ha, $\delta E_{\mathrm{tol}} = 0.28$ Ha, $r_{\mathrm{cut}} = 0.54\, r_{\mathrm{WS}}$, and $n_{\mathrm{step}} = 6000$. The error bars represent the standard deviation.

It turns out that a plateau, i.e., a domain of time where the fluctuations of $D_{\mathrm{GK}}(t)$ around its mean value are small compared to the standard deviation, is easily obtained for $D_{\mathrm{GK}}(t)$. The final graphs obtained for the cases of Table I are shown in Figs. 1–4, where the areas around the curves result from displaying the standard deviation at each t. The standard deviation increases with t, since one integrates the statistical error together with the exact signal, and varies roughly like $\sqrt{t}$. The value of D, indicated by a horizontal line, is obtained by averaging the value of $D_{\mathrm{GK}}(t)$ between the time when the velocity autocorrelation function (averaged over the atoms) first cancels and $n_{\mathrm{step2}}\Delta t$; the standard deviation of D is evaluated by averaging the standard deviation of $D_{\mathrm{GK}}(t)$ over the same interval indicated by the horizontal line. In practice, both D and its standard deviation depend little on the interval of time chosen for averaging.

The variation of D with respect to n_{step} and Δt, which govern the exploration of the phase space, and to N and r_{cut},

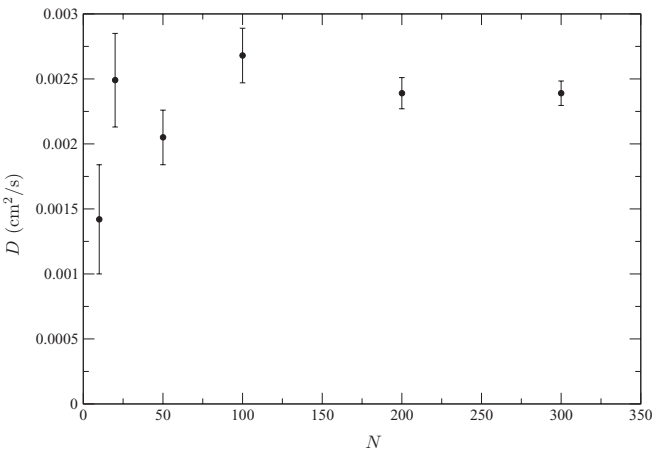

FIG. 7. Variation of the self-diffusion coefficient D with respect to N for B_1. The numerical parameters are $\Delta t = 12.53$ a.u., $e_{\mathrm{cut}} = 50$ Ha, $r_{\mathrm{cut}} = 0.54\, r_{\mathrm{WS}}$, and $n_{\mathrm{step}} = 6000$; here δE_{tol} is taken proportional to N with $\delta E_{\mathrm{tol}} = 0.28$ Ha for $N = 300$. The error bars represent the standard deviation.

TABLE II. Self-diffusion coefficient D and its standard deviation in parentheses, obtained by TFDMD. $\tilde{D}$ is obtained by the Daligault fit [27] used with Z_{eff}, defined in Eq. (17), instead of Z.

Element	D (cm^2/s)	$\tilde{D}$ (cm^2/s)
B_1	2.39×10^{-3} (9.4×10^{-5})	2.33×10^{-3}
B_2	1.60×10^{-2} (6.9×10^{-4})	1.68×10^{-2}
Cu	4.07×10^{-3} (2.0×10^{-4})	4.06×10^{-3}
D	1.59×10^{-2} (5.8×10^{-4})	1.42×10^{-2}

which characterize the system periodicity and the nucleus-electron interaction, is shown in Figs. 5–8 for B_1. It appears that convergence is obtained, within one standard deviation, for n_{step} equal to a few thousand and $N = 20$ (we have retained $N = 300$ to get a smaller statistical error). A rapid change occurs in the variation of D with N at $N \simeq 10$ and with Δt at $\Delta t \simeq 50$ a.u. The standard deviation is about 4% of D; for given thermodynamic conditions, it depends mainly on N and essentially in $1/\sqrt{N}$. That the standard deviation $\sigma(D)$ of D depends little on n_{step} comes from our process of evaluation; in fact, for a given t, $\sigma[D_{\text{GK}}(t)]$ depends indeed on n_{step} but, as $\sigma(D)$ is evaluated by averaging $\sigma[D_{\text{GK}}(t)]$ over an interval of length $n_{\text{step2}}\Delta t$ and as $\sigma[D_{\text{GK}}(t)]$ increases with t, the decrease with n_{step} at given t is roughly compensated by the increase of the domain of integration. Similar results have been found for the other cases treated in the present work; the values of D and of its standard deviation for these cases are given in Table II.

B. Viscosity

Unlike the self-diffusion coefficient, which involves averaging over the atoms, viscosity depends on the whole system so that long trajectories are necessary to improve statistical accuracy; as a consequence, viscosity is generally obtained by extrapolation of the off-diagonal stress tensor autocorrelation function [5] or of its partial integral [1,7,8], which gives rise to an unknown error. In the present work, in order to get rid of this error, we do not resort to extrapolation. The function

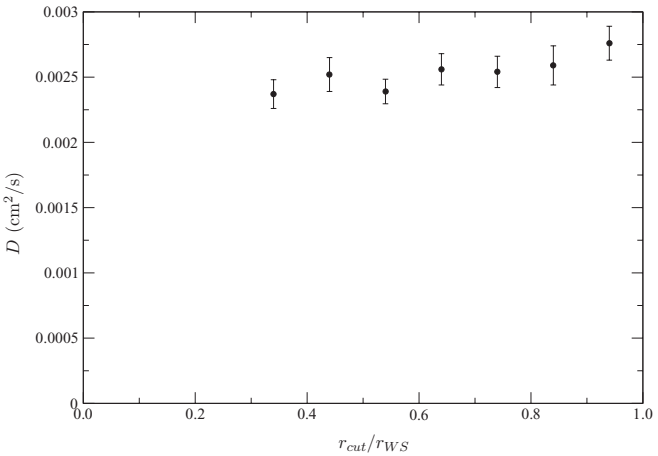

FIG. 8. Variation of the self-diffusion coefficient D with respect to r_{cut} for B_1. The numerical parameters are $N = 300$, $\Delta t = 12.53$ a.u., $\delta E_{\text{tol}} = 0.28$ Ha, and $n_{\text{step}} = 6000$ (e_{cut} varies with r_{cut}). The error bars represent the standard deviation.

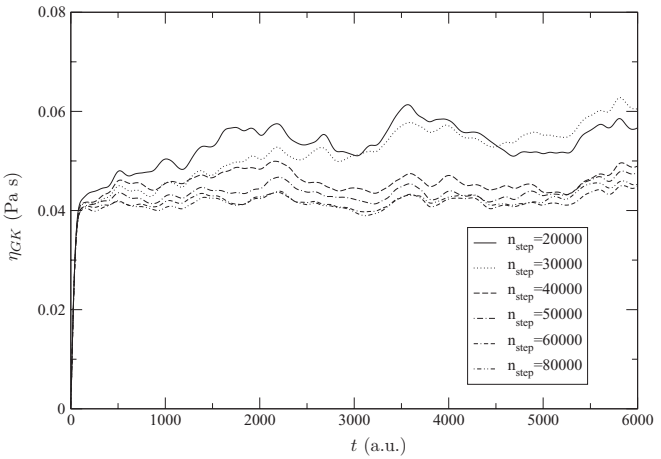

FIG. 9. Sensitivity of $\eta_{\text{GK}}(t)$ to n_{step} for Cu. The numerical parameters are $N = 20$, $\Delta t = 6.92$ a.u., $e_{\text{cut}} = 100$ Ha, $r_{\text{cut}} = 0.37\, r_{\text{WS}}$, and $\delta E_{\text{tol}} = 10^{-6}$ Ha. The standard deviation is not represented.

$\eta_{\text{GK}}(t)$ is expected to be a constant in the $t \to +\infty$ limit, and this constant is equal to the viscosity η. The search for the right numerical parameters is carried out as indicated for the self-diffusion coefficient but the new aspect here is that it is difficult to obtain a plateau [i.e., a domain of time where the fluctuations of $\eta_{\text{GK}}(t)$ around its average are small compared to the standard deviation] for the curve $\eta_{\text{GK}}(t)$. We have found that the possibility of obtaining a plateau is sensitive to the choice of n_{step}; as illustrated in Fig. 9 for Cu, increasing n_{step} tends to straighten $\eta_{\text{GK}}(t)$. Let t_p designate the time at which the first maximum of $\eta_{\text{GK}}(t)$ occurs. We have proceeded by increasing n_{step}, with all the other parameters fixed, until the curve $\eta_{\text{GK}}(t)$ shows a plateau, mainly independent of n_{step} (within one standard deviation), with a length of the order of t_p at least. With this choice of n_{step}, in the four cases treated, we have found it possible to choose numerical parameters giving a plateau with a length of the order of t_p, and to verify that the value of this plateau has indeed converged (within one standard

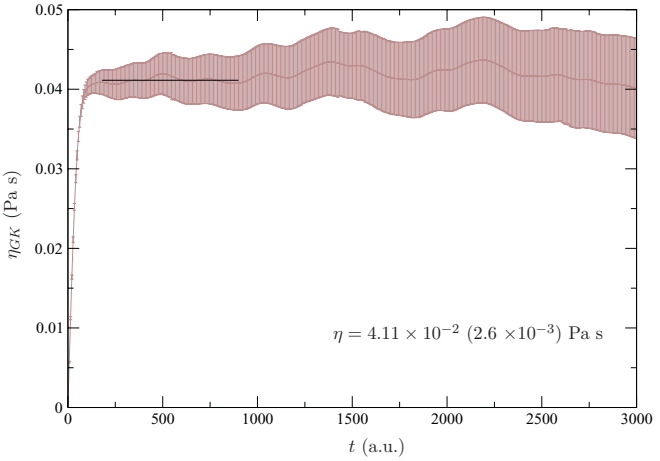

FIG. 10. (Color online) $\eta_{\text{GK}}(t)$ for Cu. The numerical parameters are $N = 20$, $\Delta t = 6.92$ a.u., $e_{\text{cut}} = 100$ Ha, $\delta E_{\text{tol}} = 10^{-6}$ Ha, $r_{\text{cut}} = 0.37\, r_{\text{WS}}$, and $n_{\text{step}} = 60\,000$. The horizontal line indicates the domain of time used to calculate η and its standard deviation (written in parentheses). The error bars represent the standard deviation.

TABLE III. Viscosity η and its standard deviation in parentheses, obtained by TFDMD. $\tilde{\eta}$ is obtained by the Bastea fit [28] used with Z_{eff}, defined in Eq. (17), instead of Z.

Element	η (Pa s)	$\tilde{\eta}$ (Pa s)
B_1	3.57×10^{-3} (2.2×10^{-4})	3.59×10^{-3}
B_2	9.18×10^{-4} (1.2×10^{-4})	1.07×10^{-3}
Cu	4.11×10^{-2} (2.6×10^{-3})	4.22×10^{-2}
D	1.23×10^{-3} (1.2×10^{-4})	1.34×10^{-3}

deviation) with respect to the parameters. The common domain of time over which $\eta_{\text{GK}}(t)$ remains mainly constant for all the (sufficiently large or small) parameters considered is used to average $\eta_{\text{GK}}(t)$ and its standard deviation; it is thus implicitly assumed that the stress tensor autocorrelation function no longer contributes to the viscosity beyond this domain (whose length is of the order of t_p in practice). The curve $\eta_{\text{GK}}(t)$ finally found for Cu is shown in Fig. 10, where the domain of time used to average $\eta_{\text{GK}}(t)$ and its standard deviation is indicated by a horizontal line. The sensitivity of $\eta_{\text{GK}}(t)$ to N and r_{cut} is shown in Figs. 11 and 12. The variation of η with N and r_{cut} is shown in Figs. 13 and 14.

The curves $\eta_{\text{GK}}(t)$ finally obtained for the three other cases of Table I are shown in Figs. 15–17. The values of η and of its standard deviation are given in Table III. For the four cases treated, numerical convergence is obtained, within one standard deviation, for N equal to 20 and n_{step} equal to a few tens of thousand. The standard deviation of η is here between 6 and 13% of η. As in the case of diffusion, the standard deviation of $\eta_{\text{GK}}(t)$ increases with t and varies roughly like $\sqrt{t}$; a variation like approximately $\sqrt{t}$ has also been obtained by Alfè and Gillan for liquid aluminum and liquid iron-sulfur [6]. We have also found that this standard deviation varies like $1/\sqrt{n_{\text{step}}\,\Delta t}$; an explanation of this variation can be found in Ref. [25]. As t increases, the standard deviation of $\eta_{\text{GK}}(t)$ can therefore be controlled by increasing n_{step}. We have verified that the values of $\eta_{\text{GK}}(t)$ obtained at any time are compatible within statistical error with the value of η calculated.

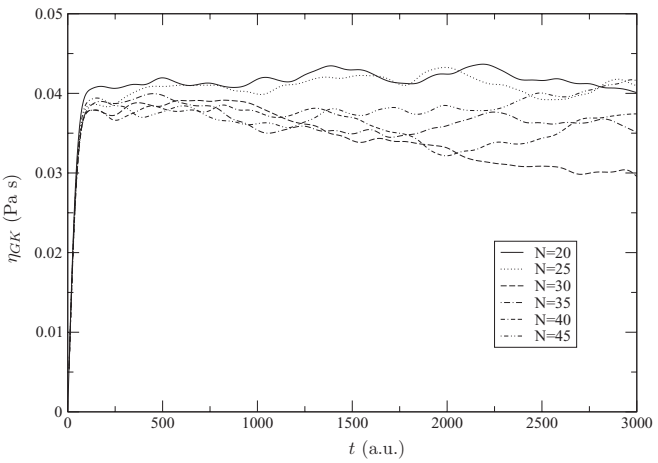

FIG. 11. Sensitivity of $\eta_{\text{GK}}(t)$ to N for Cu. The numerical parameters are $\Delta t = 6.92$ a.u., $e_{\text{cut}} = 100$ Ha, $\delta E_{\text{tol}} = 10^{-6}$ Ha, $r_{\text{cut}} = 0.37\ r_{\text{WS}}$, and $n_{\text{step}} = 60\,000$. The standard deviation is not represented.

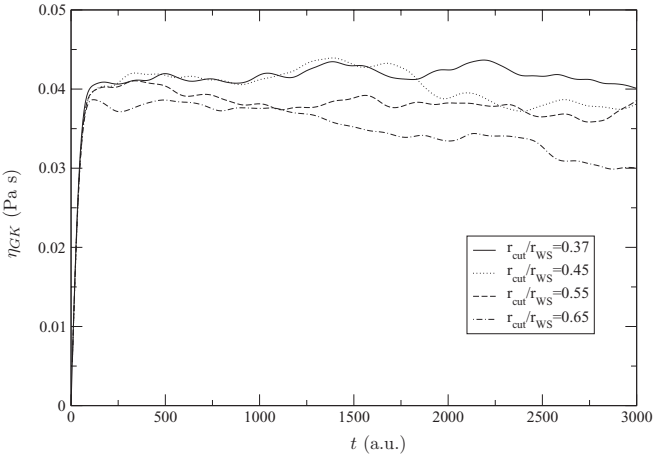

FIG. 12. Sensitivity of $\eta_{\text{GK}}(t)$ to r_{cut} for Cu. The numerical parameters are $N = 20$, $\Delta t = 6.92$ a.u., $e_{\text{cut}} = 100$ Ha, $\delta E_{\text{tol}} = 10^{-6}$ Ha, $n_{\text{step}} = 60\,000$ for $r_{\text{cut}}/r_{\text{WS}} = 0.37$ and $r_{\text{cut}}/r_{\text{WS}} = 0.45$, $n_{\text{step}} = 80\,000$ for $r_{\text{cut}}/r_{\text{WS}} = 0.55$, and $n_{\text{step}} = 100\,000$ for $r_{\text{cut}}/r_{\text{WS}} = 0.65$. The standard deviation is not represented.

It is interesting to observe what results are obtained when the partial integral of the off-diagonal stress tensor autocorrelation function, assumed to be proportional to $1-\exp(-t/\tau)$, is extrapolated to the $t \to +\infty$ limit. Here, the partial integral computed is fitted over the interval $[0,t_{\text{ex}}]$ with three possible values of t_{ex} defined by $\eta_{\text{GK}}(t_{\text{ex}}) = 0.63\eta$, 0.86η, or 0.95η (respectively corresponding to $t_{\text{ex}} = \tau$, 2τ, or 3τ with the exponential time dependence assumed). The viscosities thus obtained are given in Table IV, where it appears that a viscosity calculated by extrapolation can be very different from the exact result. This is so in the cases B_1 and Cu (Table IV) whereas, in the cases B_2 and D (Table IV), the viscosity obtained by extrapolation is in agreement, within one standard deviation, with the exact result. The apparent difference between the cases B_1 and Cu on the one hand and B_2 and D on the other hand is the number of time steps in the fitting interval $[0,t_{\text{ex}}]$ (for instance, when $t_{\text{ex}} = \tau$, 6 for B_1 and Cu, 24 for B_2, and 27 for D). However, for Cu and B_2, for instance, we have found by changing Δt that the difference of agreement between the exact result and the extrapolation result remains even when the same number of time steps (12) is used in $[0,t_{\text{ex}} = \tau]$. Therefore it is not the number of time steps in the fitting interval but rather the shape of $\eta_{\text{GK}}(t)$ that causes the difference of agreement. This observation leads us to suggest caution about the extrapolation approach.

TABLE IV. Viscosity (in Pa s) obtained by extrapolation of the partial integral of the off-diagonal stress tensor autocorrelation function, assumed to be proportional to $[1-\exp(-t/\tau)]$, fitted on the interval $[0,t_{\text{ex}}]$.

Element	$t_{\text{ex}} = \tau$	$t_{\text{ex}} = 2\tau$	$t_{\text{ex}} = 3\tau$
B_1	7.11×10^{-3}	5.19×10^{-3}	4.42×10^{-3}
B_2	8.69×10^{-4}	9.03×10^{-4}	9.03×10^{-4}
Cu	8.15×10^{-2}	5.93×10^{-2}	5.05×10^{-2}
D	1.17×10^{-3}	1.22×10^{-3}	1.25×10^{-3}

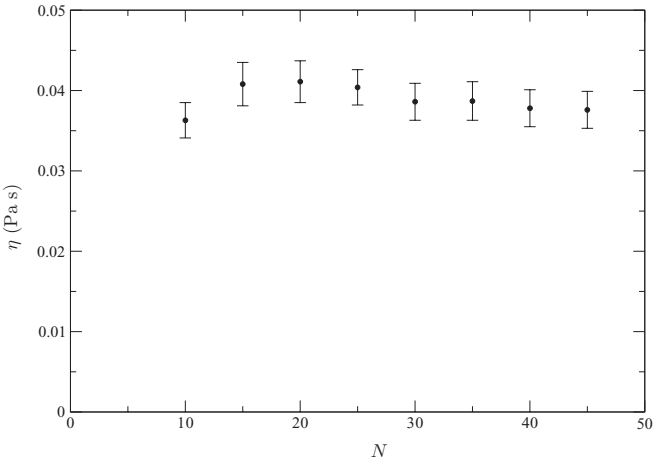

FIG. 13. Variation of the viscosity η with respect to N for Cu. The numerical parameters are $\Delta t = 6.92$ a.u., $e_{\rm cut} = 100$ Ha, $\delta E_{\rm tol} = 10^{-6}$ Ha, $r_{\rm cut} = 0.37\, r_{\rm WS}$, and $n_{\rm step} = 60\,000$. The error bars represent the standard deviation.

IV. APPROXIMATION BY SIMPLE MODELS

We now compare the transport coefficients obtained above by TFDMD to the results given by simple analytical models. The self-diffusion coefficient and viscosity are usually expressed as dimensionless quantities D^* and η^* defined by

$$D^* = \frac{D}{\omega_p\, r_{\rm WS}^2}, \tag{14}$$

$$\eta^* = \frac{\eta}{n_i\, m\, \omega_p\, r_{\rm WS}^2}, \tag{15}$$

where m is the mass of a nucleus, and the plasma frequency for ions ω_p is defined by

$$\omega_p^2 = \frac{4\pi n_i Z^2}{m}. \tag{16}$$

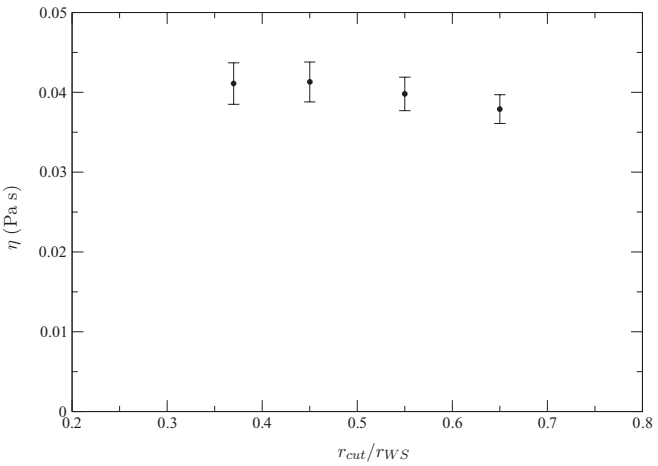

FIG. 14. Variation of the viscosity η with respect to $r_{\rm cut}$ for Cu. The numerical parameters are $N = 20$, $\Delta t = 6.92$ a.u., $e_{\rm cut} = 100$ Ha, $\delta E_{\rm tol} = 10^{-6}$ Ha, $n_{\rm step} = 60\,000$ for $r_{\rm cut}/r_{\rm WS} = 0.37$ and $r_{\rm cut}/r_{\rm WS} = 0.45$, $n_{\rm step} = 80\,000$ for $r_{\rm cut}/r_{\rm WS} = 0.55$, and $n_{\rm step} = 100\,000$ for $r_{\rm cut}/r_{\rm WS} = 0.65$. The error bars represent the standard deviation.

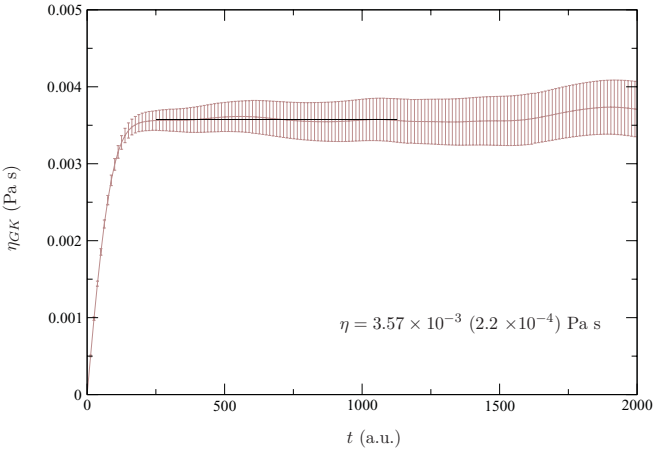

FIG. 15. (Color online) $\eta_{\rm GK}(t)$ for B_1. The numerical parameters are $N = 20$, $\Delta t = 12.53$ a.u., $e_{\rm cut} = 50$ Ha, $\delta E_{\rm tol} = 2\ 10^{-7}$ Ha, $r_{\rm cut} = 0.54\, r_{\rm WS}$, and $n_{\rm step} = 40\,000$. The horizontal line indicates the domain of time used to calculate η and its standard deviation (written in parentheses). The error bars represent the standard deviation.

Lambert *et al.* [12] have proposed to calculate the self-diffusion coefficient and viscosity by using the one component plasma (OCP) model [26] with an effective atomic number $Z_{\rm eff}$ defined by

$$Z_{\rm eff} = \tfrac{4}{3}\pi\, r_{\rm WS}^3\, n_{\rm AA}(r_{\rm WS}), \tag{17}$$

where $n_{\rm AA}(r_{\rm WS})$ is the electronic density at the atom surface in the average-atom model [9] for the thermodynamic conditions considered.

Here, in a similar way, we calculate an approximate value of the self-diffusion coefficient, $\tilde{D}$, by using the Daligault fit of D^* for the OCP [27] with $Z_{\rm eff}$ instead of Z. Likewise, for viscosity, we calculate an approximate value $\tilde{\eta}$ by using the Bastea fit of η^* for the OCP [28] with $Z_{\rm eff}$ instead of Z. The results, given in Tables II and III, turn out to be in good agreement with the values obtained by TFDMD over a range

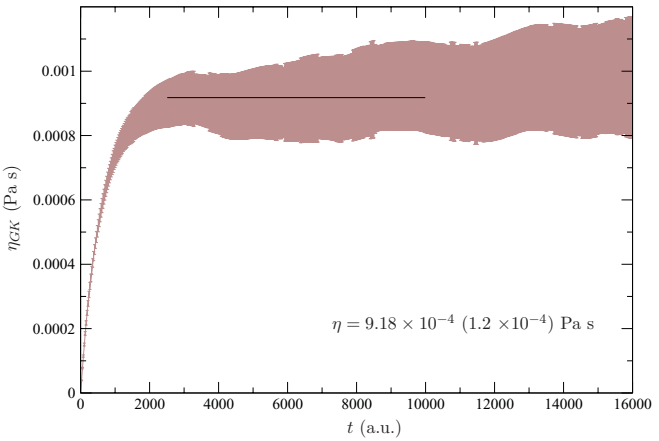

FIG. 16. (Color online) $\eta_{\rm GK}(t)$ for B_2. The numerical parameters are $N = 20$, $\Delta t = 27$ a.u., $e_{\rm cut} = 40$ Ha, $\delta E_{\rm tol} = 2\ 10^{-7}$ Ha, $r_{\rm cut} = 0.35\, r_{\rm WS}$, and $n_{\rm step} = 40\,000$. The horizontal line indicates the domain of time used to calculate η and its standard deviation (written in parentheses). The error bars represent the standard deviation.

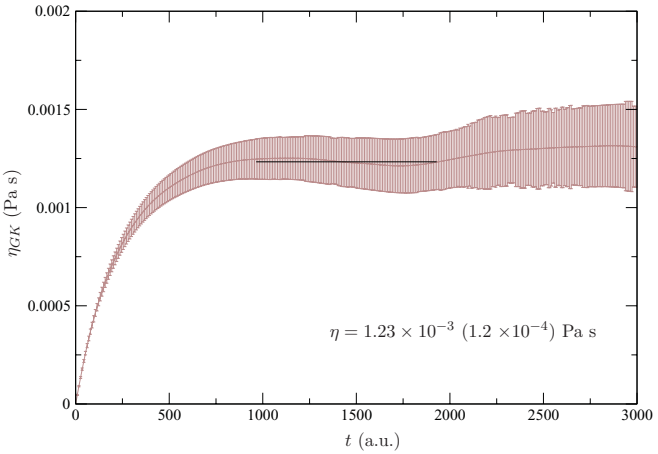

FIG. 17. (Color online) $\eta_{\mathrm{GK}}(t)$ for D. The numerical parameters are $N = 20$, $\Delta t = 8.77$ a.u., $e_{\mathrm{cut}} = 90$ Ha, $\delta E_{\mathrm{tol}} = 10^{-6}$ Ha, $r_{\mathrm{cut}} = 0.59\, r_{\mathrm{WS}}$, and $n_{\mathrm{step}} = 40\,000$. The horizontal line indicates the domain of time used to calculate η and its standard deviation (written in parentheses). The error bars represent the standard deviation.

of coupling constants between 7 and 170 (between 2.4 and 23 if calculated with Z_{eff} instead of Z).

V. CONCLUSION

In the framework of OFMD at the Thomas-Fermi-Dirac level, we have carried out an extensive study of the numerical convergence of the self-diffusion coefficient D and viscosity η, calculated by the Green-Kubo formula, in four cases covering a large domain of coupling constant. We have shown that it is possible to calculate the viscosity by OFMD at the Thomas-Fermi-Dirac level without resorting to the extrapolation of the off-diagonal stress tensor autocorrelation function, thereby eliminating the unknown error due to extrapolation; the key point in obtaining a plateau for $\eta_{\mathrm{GK}}(t)$ is to sufficiently increase the number of time steps used in the calculation. Convergence for viscosity is reached at $N = 20$ per basic cell and at n_{step} equal to a few tens of thousand; for the self-diffusion coefficient, convergence is reached at $N = 200$ or 300 (or smaller N if larger statistical errors are accepted) and at n_{step} equal to a few thousand. For given thermodynamic conditions, and with our conventions for calculating D and η, the standard deviation of D varies mainly with the number of atoms in the basic cell N, essentially in $1/\sqrt{N}$, and the standard deviation of η varies mainly with the number n_{step} of time steps and with the time step Δt, essentially in $1/\sqrt{(n_{\mathrm{step}}\, \Delta t)}$.

We have found that extrapolating the partial integral of the off-diagonal stress tensor autocorrelation function may lead to large errors; we therefore suggest caution about using extrapolation in the calculation of viscosity.

Finally, for the cases considered (which cover a large domain of coupling constant), the self-diffusion and viscosity are well approximated, respectively, by the Daligault fit [27] and by the Bastea fit [28] used with a single effective atomic number calculated with the average-atom model.

ACKNOWLEDGMENTS

The present results have been obtained through the use of the ABINIT code, a common project of the Université Catholique de Louvain, Corning Incorporated, and other contributors (see http://www.abinit.org).

[1] J. D. Kress, J. S. Cohen, D. A. Horner, F. Lambert, and L. A. Collins, Phys. Rev. E **82**, 036404 (2010).
[2] U. Gupta and A. K. Rajagopal, Phys. Rep. **87**, 260 (1982).
[3] I. Kwon, J. D. Kress, and L. A. Collins, Phys. Rev. B **50**, 9118 (1994).
[4] J. G. Clérouin and S. Bernard, Phys. Rev. E **56**, 3534 (1997).
[5] J. Clérouin and J.-F. Dufrêche, Phys. Rev. E **64**, 066406 (2001).
[6] D. Alfè and M. J. Gillan, Phys. Rev. Lett. **81**, 5161 (1998).
[7] D. A. Horner, F. Lambert, J. D. Kress, and L. A. Collins, Phys. Rev. B **80**, 024305 (2009).
[8] J. D. Kress, J. S. Cohen, D. P. Kilcrease, D. A. Horner, and L. A. Collins, Phys. Rev. E **83**, 026404 (2011).
[9] F. Perrot, Phys. Rev. A **20**, 586 (1979).
[10] R. G. Parr and W. Yang, *Density-Functional Theory of Atoms and Molecules* (Oxford University Press, New York, 1989).
[11] G. Zérah, J. G. Clérouin, and E. L. Pollock, Phys. Rev. Lett. **69**, 446 (1992).
[12] F. Lambert, J. Clérouin, and S. Mazevet, Europhys. Lett. **75**, 681 (2006).
[13] F. Lambert, J. Clérouin, J.-F. Danel, L. Kazandjian, and G. Zérah, Phys. Rev. E **77**, 026402 (2008).
[14] J. D. Kress, J. S. Cohen, D. P. Kilcrease, D. A. Horner, and L. A. Collins, High Energy Density Phys. **7**, 155 (2011).
[15] X. Gonze *et al.*, Comput. Mater. Sci. **25**, 478 (2002).
[16] X. Gonze *et al.*, Z. Kristallogr. **220**, 558 (2005).
[17] J. P. Perdew and A. Zunger, Phys. Rev. B **23**, 5048 (1981).
[18] F. Zhang, J. Chem. Phys. **106**, 6102 (1997).
[19] P. Minary, G. J. Martyna, and M. E. Tuckerman, J. Chem. Phys. **118**, 2510 (2003).
[20] O. H. Nielsen and R. M. Martin, Phys. Rev. B **32**, 3792 (1985).
[21] F. Lambert, J. G. Clérouin, and G. Zérah, Phys. Rev. E **73**, 016403 (2006).
[22] J.-F. Danel, L. Kazandjian, and G. Zérah, Phys. Plasmas **13**, 092701 (2006).
[23] J. M. Haile, *Molecular Dynamics Simulation* (Wiley-Interscience, New York, 1997).
[24] M. P. Allen and D. J. Tildesley, *Computer Simulation of Liquids* (Oxford Science Publications, Oxford, 1987).
[25] R. Zwanzig and N. K. Ailawadi, Phys. Rev. **182**, 280 (1969).
[26] J.-P. Hansen, Phys. Rev. A **8**, 3096 (1973).
[27] J. Daligault, Phys. Rev. Lett. **96**, 065003 (2006); **103**, 029901(E) (2009).
[28] S. Bastea, Phys. Rev. E **71**, 056405 (2005).